Journal of Catalysis **196,** 115–125 (2000)
doi:10.1006/jcat.2000.3030, available online at http://www.idealibrary.com on IDEAL®

Heats of Adsorption of Linear and Multibound Adsorbed CO Species on a Pt/Al_2O_3 Catalyst Using *in Situ* Infrared Spectroscopy under Adsorption Equilibrium

Abdennour Bourane, Olivier Dulaurent, and Daniel Bianchi[1]

Laboratoire d'Application de la Chimie à l'Environnement (LACE), UMR 5634, Université Claude Bernard, Lyon-I, Bat. 308, 43 Bd du 11 Novembre 1918, 69622 Villeurbanne, France

Received April 19, 2000; revised August 7, 2000; accepted August 7, 2000

The adsorption of CO (1 and 10% CO/He mixtures, 1 atm total pressure) on a reduced 2.9% Pt/Al_2O_3 catalyst in the temperature range 298–740 K is studied using Fourier transform infrared spectroscopy (FTIR). Several adsorbed CO species on Pt sites are detected at 300 K: linear (IR band at 2075 cm^{-1}), bridged (three species; IR bands at 1878, 1835, and 1824 cm^{-1}), and threefold coordinated CO species (IR band at 1800 cm^{-1}) which are denoted by L, B, and 3FC, respectively. The evolution of the intensities of the IR bands with the adsorption temperature T_a allows the determination of the change of the coverage θ of each adsorbed CO species with T_a. The curves $\theta = f(T_a)$ permit the determination of the heats of adsorption of the three adsorbed species using the same adsorption model which considers: (a) a linear decrease in the heats of adsorption E_θ as a function of θ; and (b) immobile adsorbed species. The following heat of adsorption values were found (the subscript indicates the value of the coverage): for the L species, $E\mathbf{L}_0 = 206$ kJ/mol and $E\mathbf{L}_1 = 115$ kJ/mol; for the B species, $E\mathbf{B}_0 = 94$ kJ/mol and $E\mathbf{B}_1 = 45$ kJ/mol; for the 3FC species, $E\mathbf{3FC}_0 = 135$ kJ/mol and $E\mathbf{3FC}_1 = 104$ kJ/mol. In order to validate the assumptions of the adsorption model, the heats of adsorption obtained with the present procedure are compared to the isosteric heat of adsorption for the L and B species.

Key Words: **carbon monoxide; chemisorption; platinum; FTIR; heat of adsorption, adsorption model.**

1. INTRODUCTION

The heats of adsorption of the adsorbed species (denoted by E) and their evolutions with the coverage θ (denoted by E_θ with $0 \le \theta \le 1$) constitute a fundamental parameter for characterization of the CO/metal systems because the values of E_θ quantify the coverage of the sites (according to classical definitions (1, 2)) under adsorption equilibrium. However, this parameter is rarely studied on supported metal catalysts due to experimental difficulties. For instance, temperature-programmed desorption methods (TPD) that permit determination of the desorption activation energies (usually equal to E_θ for the CO/noble metal systems) on single crystals are not well adapted for supported metal catalysts because it is difficult to achieve TPD experimental conditions free of the influence of diffusion and readsorption (3, 4). This explains the interest in microcalorimetric methods (5, 6), which provide either the integral or the differential heat of adsorption. However, in the case of the formation of several adsorbed CO species, for instance linear (denoted by L) and bridged (denoted by B) CO species, this method provides an average of the heats of adsorption. The E_θ values can be also determined using the Clausius–Clapeyron equation from the amount of the adsorbed CO species measured for several adsorption pressures and temperatures (7). The accuracy of the experimental method providing the adsorbed quantities must be very high otherwise, the values of the heats of adsorption are strongly affected. Moreover, the analytical methods must be able to differentiate the amount of each adsorbed species or else, at best, only an average of the heats of adsorption can be obtained. This is the case for single crystals and supported model particles using IRAS spectroscopy. This analytical method permits characterization of each adsorbed CO species by their IR bands and the isosteric heats of adsorption of well identified adsorbed species have been determined (8, 9). We have shown previously (10–14) that the evolution of the intensities of the IR bands of the adsorbed CO species on supported metal catalysts: Pd (L and B species) (10), Pt (L species) (11, 12), Ru (L species) (13), Rh (L and B species) (14) with the adsorption temperature T_a for a given CO partial pressure P_a leads to the determination of the change in the coverage θ of each adsorbed species with T_a. The curves $\theta = f(T_a)$ allow determination of the heats of adsorption of the various adsorbed species using an adsorption model (10–14). The heats of adsorption obtained with this procedure for the L species on a Pt/Al_2O_3 catalyst were in good agreement with the isosteric heat of adsorption determined using several isobars (12). The first objective of the present study is to show that

[1] To whom correspondence should be addressed. E-mail: daniel.bianchi@univ-lyon1.fr.

0021-9517/00 $35.00

the above method can also be used for the determination of the heats of adsorption of B and threefold coordinated (denoted by 3FC) CO species on the same Pt/Al_2O_3 catalyst. It is shown that the heats of adsorption of the B species are significantly lower than that of the L species, leading to the conclusion that on a Pt/Al_2O_3 catalyst and for given T_a and P_a values, the coverage of the Pt sites adsorbing the B species can be very low while that of the sites adsorbing the L species is equal to 1. This means that in the course of a catalytic reaction involving CO, the Pt sites adsorbing the B species are partially free for the adsorption of a second gas while the other sites can be fully covered with CO.

2. EXPERIMENTAL

The 2.9% Pt/Al_2O_3 (in wt%) catalyst was prepared by the incipient wetness method. Alumina (Degussa C γ-Al_2O_3, BET area 100 m^2/g) was impregnated using an amount of aqueous solution of H_2PtCl_6, xH_2O (Aldrich). After drying for 12 h at room temperature and then for 24 h at 373 K, the solid was treated for 12 h in air at 713 K. The noble metal content was obtained using the inductively coupled plasma method after dissolution of the catalyst powder. For the FTIR study, the catalyst was compressed to form a disk ($\Phi = 1.8$ cm) which was placed in the sample holder of a small internal volume stainless steel IR cell (transmission mode) described elsewhere (11). This IR cell enabled *in situ* treatments (293–900 K) of the solid, at atmospheric pressure, with a gas flow rate in the range of 150–2000 cm^3/min. Before the adsorption of CO, the solid was treated *in situ* (150 cm^3/min) according to the following procedure: oxygen ($T = 713$ K, $t = 30$ min) $\rightarrow$ helium ($T = 713$ K, $t = 30$ min) $\rightarrow$ hydrogen ($T = 713$ K, $t = 1$ h) $\rightarrow$ helium ($T = 713$ K, $t = 10$ min) $\rightarrow$ helium (adsorption temperature). After this treatment, the dispersion of the metallic phase of the reduced catalyst using the adsorption of CO at 300 K and assuming a ratio CO/M = 1 was 85%, in agreement with literature data (6) on similar Pt catalysts. The same catalyst pellet was used for several experiments and it was pretreated before each adsorption experiment as described above. The data were obtained according to the following procedure: after the pretreatment of the solid, a x% CO/He mixture (Total pressure = 1 atm, $x = 1$ or 10, flow rate = 200 cm^3/min) was introduced in the IR cell at 300 K and then T_a was slowly increased ($\approx$5–10 K/min) up to 740 K while the FTIR spectra of the adsorbed species were recorded periodically. Then the solid was cooled down to a temperature T in the presence of 1% CO/He and the FTIR spectrum was compared with the spectrum recorded at a similar temperature in the course of the heating stage. This comparison revealed the modifications of the surface in the course of the adsorption such as poisoning of the surface by the carbon deposition coming from the dissociation/disproportionation reaction of CO. An irreversible aging of the catalyst was observed after the first adsorption of 1% CO/He, at 740 K, leading to a decrease by 13% of the IR band of the linear species recorded at 300 K compared with a fresh catalyst. After this modification two consecutive experiments, adsorption of 1% CO/He at $\approx$740 K/pretreatment, provided IR bands with similar intensities after adsorption of CO at 300 K and the catalyst is considered as stabilized. The aging, however, continued with a low rate as indicated by the decrease by 10% between the 2nd and the 10th cycle. All the results presented were obtained on an aged solid but which has been used for less than 10 cycles. The IR spectra in the range 2000–1700 cm^{-1} indicated the superposition of several IR bands due to the presence of several adsorbed CO species. The purpose of the present paper imposed the determination of the contribution of each type of adsorbed species to the FTIR spectra. This was achieved using a deconvolution method (see below) based on the difference in the stability of the adsorbed species.

3. RESULTS AND DISCUSSION

The main objective of the present study is the determination and the comparison of the heats of adsorption of the L, B, and 3FC CO species adsorbed on reduced platinum particles of the 2.9% Pt/Al_2O_3 catalyst under adsorption equilibrium conditions. The results for the linear CO species have been described in detail previously (11, 12) and the main results are briefly summarized below to facilitate the comparison with B and 3FC species which have not been described for now.

3.1. IR Spectra after Adsorption of CO at 300 K on Reduced Pt/Al_2O_3

Figure 1 (spectrum a) shows the IR bands of the adsorbed CO species on the stabilized and reduced 2.9% Pt/Al_2O_3 catalyst using a 1% CO/He mixture at 300 K. The strong IR band at 2075 cm^{-1} and the broad weak IR band at $\approx$1830 cm^{-1} are ascribed to L and multibound CO species (B/3FC), respectively (15–18). They are several L and B species which can be simultaneously present after adsorption of CO on Pt-containing solids leading to different IR bands (15 and references therein). Xu and Yates (19) using IRAS spectroscopy have shown that the adsorption of CO on Pt(335) and Pt(112) may lead to four IR bands (two above and two below 2000 cm^{-1}) assigned to L and B species on steps and on terraces. For instance, for the L species an IR band at $\approx$2070 cm^{-1} is ascribed to CO on steps and an IR band at 2090 cm^{-1} to CO on terraces. On the present catalyst the position of the IR band at 2075 cm^{-1} on the highly dispersed Pt particles is in agreement with the assignment of L species on step. The weak intensity of the IR band of the multibound CO species in Fig. 1a compared with that of the linear CO species does not indicate necessarily that the

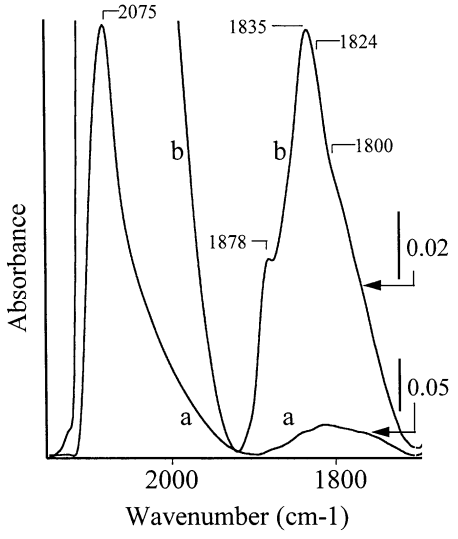

FIG. 1. FTIR spectra recorded at 300 K on reduced stabilized 2.9% Pt/Al_2O_3 solid with the 1% CO/He mixture: (a) low weight pellet of catalyst; (b) high weight pellet of catalyst.

amount of B/3FC species on the surface is much lower than that of the L species if it is considered that the extinction absorption coefficient of the L species ε_L is higher than that of the B species ε_B (20).

The low intensities of the IR bands in the 1900–1700 cm^{-1} range in Fig. 1a does not allow us to characterize clearly the B/3FC species. Spectrum b in Fig. 1 is obtained under the same experimental conditions (stabilized and reduced solid) but with a 2.8-times-heavier disk of catalyst than used in Fig. 1a. Under these conditions there is no transmission at the maximum of the IR band of the L species. Figure 1b shows that in the 1900–1700 cm^{-1} range there is an overlap of several IR bands leading to a shoulder at 1878 cm^{-1}, an IR band at 1835 cm^{-1}, a small shoulder at 1824 cm^{-1}, and a broad shoulder at $\approx$1800 cm^{-1}. These IR bands indicate that there are several B species on the Pt surface. Xu and Yates (19) assign an IR band at 1880 cm^{-1} on Pt(335) to bridged CO species formed on step sites while an IR band at 1910 cm^{-1} is assigned to bridged CO species adsorbed on terrace sites. On Pt(112) the authors (19) observe a single IR band at 1845 cm^{-1}. Further, Haaland (22) observed on Pt/Al_2O_3 solids (a) a shoulder at 1840 cm^{-1} associated with a broad IR band at 1800 cm^{-1}; and (b) a splitting of the two IR bands in the course of an isothermal desorption at 502 K. The same results have been observed by Barth *et al.* (15) on several Pt/Al_2O_3 catalysts. Haaland (22) assigns (a) the IR band at 1800 cm^{-1} to CO in threefold coordination with Pt using the conclusions of the early work of Hayden and Bradshaw (21) for the adsorption of CO on Pt(111) and (b) the IR band at 1840 cm^{-1} to bridged CO species (22). It must be noted that Hayden and Bradshaw (21) have observed on Pt(111) that the increase in T_a leads to significant broadening of the IRAS spectra. This is in agreement with the presence of the broad shoulder at 1800 cm^{-1} in Fig. 1. Moreover, the results of Hayden and Bradshaw (21) reveal that the comparison between the profile of the IR bands observed at low temperatures on single crystals (IRAS spectroscopy) can be strongly different than those observed at high temperatures ($T > 300$ K) and this must be taken into account for the comparison of the results on single crystals at $T_a < 300$ K and on supported metal catalysts at $T_a > 300$ K. Finally considering the literature data we assign the IR bands at 1878, 1835, and 1824 cm^{-1} to three B CO species on different Pt sites situated on steps and/or defects because terrace sites lead to an IR band at a position higher than 1900 cm^{-1} (19). The broad IR band at 1800 cm^{-1} is assigned (15, 21, 22) to 3FC CO species. Note that in the present study the accurate assignment of the three B species to specific Pt sites is not a crucial problem because in the end effect these species have similar heats of adsorption (see below) whatever the coverage and this explains why we adopted the single notation B for the three adsorbed species. Spectra a and b in Fig. 1 show that the determination of the heats of adsorption of the L and B species on the Pt/Al_2O_3 solid must be performed in separate experiments with different amounts of catalyst.

3.2. Evolution of the IR Band of the L Species with T_a and Heats of Adsorption

The results observed for the linear CO species have been described in detail previously (11, 12) and are briefly summarized. Spectrum b in Fig. 2 shows that the increase in T_a with 1% CO/He on a stabilized catalyst (after two cycles adsorption of CO/pretreatment) causes the increase in intensity of the IR band of the linear CO species at temperatures lower than $\approx$460 K alongside a shift to 2067 cm^{-1} at 453 K

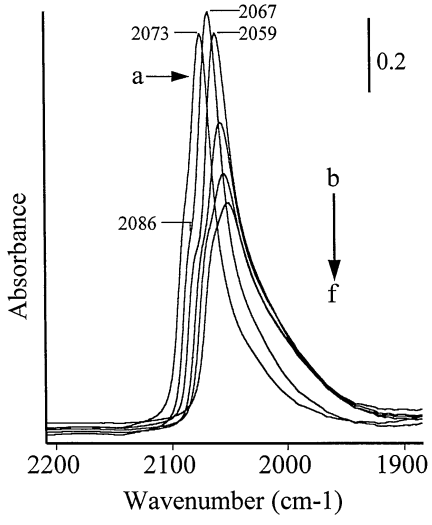

FIG. 2. Evolution of the IR band of the L CO species with the adsorption temperature using the 1% CO/He mixture: (a–f) 378 K, 453 K, 533 K, 633 K, 693 K, 783 K.

(L_1 species), while a shoulder was detected at 2086 cm^{-1} (L_2 species) at 453 K. At higher temperatures, spectra c–f in Fig. 2 lead to the following observations: (a) the shoulder shifts with the increase in T_a (2080 cm^{-1} at 533 K and 2063 cm^{-1} at 783 K); (b) the main IR band also shifts to lower wavenumbers (2061 cm^{-1} at 533 K and 2051 cm^{-1} at 783 K); (c) the IR band area (the shoulder and the main IR band are not differentiated) is constant between ≈460 and ≈580 K; and (d) the IR band area decreases at $T_a > 600$ K. The results in Fig. 2 show that the platinum surface was modified by the CO adsorption at ≈450 K (increase in intensity of the IR band and detection of the shoulder). We have suggested (11) that the origin of this modification is due to a reconstruction of the CO/Pt surface system in the presence of CO. If after adsorption at 660 K the catalyst was cooled down in the presence of 1% CO/He, the IR band area remained constant, indicating that the modification of the surface during the heating in CO was irreversible. Curve a in Fig. 3 provides at $T_a \geq 400$ K the change in the coverage θ of the Pt sites by the L species with T_a using the data in Fig. 2. The coverage is obtained using the ratio between the IR band area at T_a (the shoulder and the main IR band are not differentiated) and the highest IR band area (at $T_a \approx 540$ K) and considering that: (a) the intensity of the IR band is proportional to the amount of the linear CO species on the surface; and (b) the IR absorption extinction coefficient is independent of T_a. We showed previously (23) that these assumptions were valid for the linear CO species of the present Pt/Al_2O_3 catalyst at $T_a > 540$ K comparing the coverage of the L species using either FTIR spectroscopy or a carbon mass balance in the course of the CO adsorption using a mass spectrometer. Figure 3a shows that θ is constant between $T_a \approx 520$ K and $T_a \approx 600$ K and then decreases according to a straight line in a wide range of temperatures.

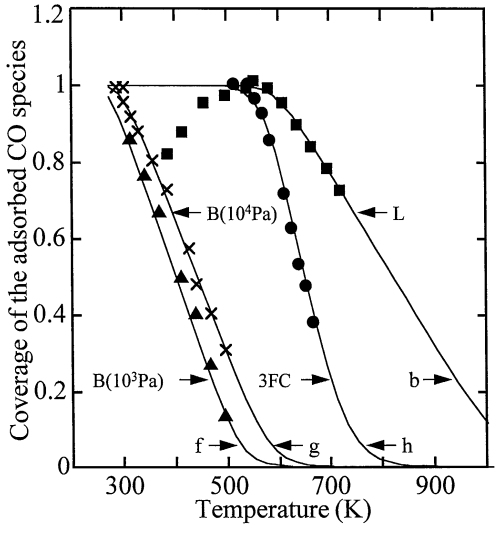

FIG. 3. Evolution of the coverage of the L and M CO species according to the adsorption temperature: ■ (a) L species, experimental data with $P_a = 10^3$ Pa; (b) L species, theoretical model; ▲ (c) B species, experimental data with $P_a = 10^3$ Pa; ✕ (d) B species, experimental data with $P_a = 10^4$ Pa; ● (e) 3FC species, experimental data with $P_a = 10^3$ Pa; (f–h) theoretical curves according the adsorption model (see the text).

The curve $\theta = f(T_a)$ at a given partial pressure can be used for the determination of the heats of adsorption of adsorbed CO species on supported metal catalysts using an adsorption model (10–14 and references therein). This model assumes that (a) the adsorbed species are immobile and (b) the heats of adsorption linearly decrease with increase in coverage. Assumption (a) makes it possible to consider that the adsorption coefficient λ (ratio of the rate constants of adsorption and desorption) is given by the statistical thermodymanics (24, 25),

$$\lambda = \frac{h^3}{k(2\pi mk)^{3/2}} \cdot \frac{1}{T_a^{5/2}} \cdot \exp\left(\frac{E_d - E_a}{RT_a}\right), \qquad [1]$$

where h is Planck's constant, k is Bolztmann's constant, m is the weight of the molecule (28×10^{-3} kg/6.02×10^{23}), T_a is the adsorption temperature, E_d and E_a are the activation energies of desorption and adsorption respectively and $E_d - E_a$ is the heat of adsorption (denoted by E). Assumption (b) leads to an expression of the coverage for an adsorbed species given by (10–14 and references therein),

$$\theta = \frac{R \cdot T_a}{\Delta E} \cdot \ln\left(\frac{1 + \lambda_0 \cdot P_a}{1 + \lambda_1 \cdot P_a}\right), \qquad [2]$$

where ΔE is the difference in the heats of adsorption at $\theta = 0$ (E_0) and $\theta = 1$ (E_1), λ_0 and λ_1 are the adsorption coefficients at $\theta = 0$ and $\theta = 1$ respectively, and T_a and P_a are the adsorption temperature and pressure, respectively. For the determination of E_1 and E_0 we only have to find the values to be used in [1] and [2] to obtain the best fit between the experimental values of the coverage and the theoretical coverage. For instance, curve b in Fig. 3 is obtained using $EL_0 = 206$ kJ/mol and $EL_1 = 115$ kJ/mol in expressions [1] and [2]. It can be observed a very good agreement between the theoretical coverage and the experimental data. We have compared (11, 12) these values with those found in the literature on single crystals, model particles, and supported metal catalysts using other analytical methods (TPD, microcalorimetry and isosteric methods) and a good agreement was observed with certain studies. In particular, Yeo *et al.* (27) determined 225 kJ/mol at $\theta \approx 0$ on Pt(100)–(1 × 1) by single crystal adsorption calorimetry method. This value is in good agreement with $EL_0 = 206$ kJ/mol. The authors (27) also observed a linear decreasing relationship from 225 kJ/mol at $\theta \approx 0$ to 195 kJ/mol at $\theta = 0.5$ and then to 80 kJ/mol at $\theta = 1$. This last value is commented below with the heats of adsorption observed for the B and 3FC species. Moreover, we have also shown that the EL values obtained with the adsorption model were in agreement with the

isosteric heats of adsorption (12) and this validated the assumptions involved in the adsorption model. Note that Liao *et al.* (26) have determined on a Pt_{10} cluster a theoretical ($X\alpha$ method) heat of adsorption of CO of 185 kJ/mol in reasonable agreement with EL_0.

3.3. Evolution of the IR Bands and of the Coverages of the B and 3FC Species with T_a

On a fresh reduced disk of catalyst (first reduction) the increase in T_a in the presence of 1% CO/He leads to an irreversible modification of the catalyst for the B/3FC species (the L species is less affected (11, 12)), as shown in Fig. 4. Spectrum a in Fig. 4 is recorded at 300 K in the presence of 1% CO/He after the first reduction of the catalyst. Spectrum b in Fig. 4, recorded at 300 K after an increase in T_a from 300 to 663 K followed by cooling of the sample in CO/He to 300 K, indicates a strong decrease in the IR band as compared to spectrum a. This shows that the adsorption of CO at high temperatures leads to a strong decrease in the number of sites adsorbing the B and 3FC species due either to a sintering of the Pt particles or to a poisoning by the C deposition due to the dissociation/disproportionation of CO. Spectrum c in Fig. 4 is recorded at 300 K on a pretreated solid after another cycle adsorption of CO at 663 K/pretreatment. Spectra a and c show that the irreversible modification of the number of Pt sites adsorbing the B and 3FC species after the first adsorption in CO (spectra a and b) is not due to C deposition. After the initial irreversible modification of the catalyst, the following cycles adsorption of CO at 663 K/pretreatment have no significant effect on the IR bands of the B and 3FC species and the catalyst is considered as stabilized. The heats of adsorption of the B and 3FC species have been determined on a stabilized solid.

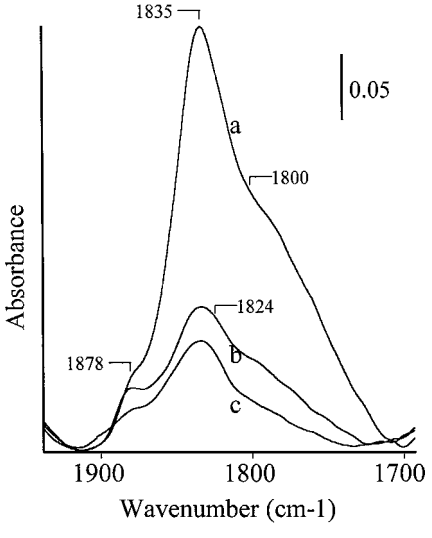

FIG. 4. Irreversible modifications of the FTIR spectra of the multibound adsorbed species with the 1% CO/He mixture at 300 K: (a) fresh reduced catalyst; (b) after adsorption at 633 K followed by cooling of the sample to 300 K; (c) after two following cycles adsorption of CO/pretreatment.

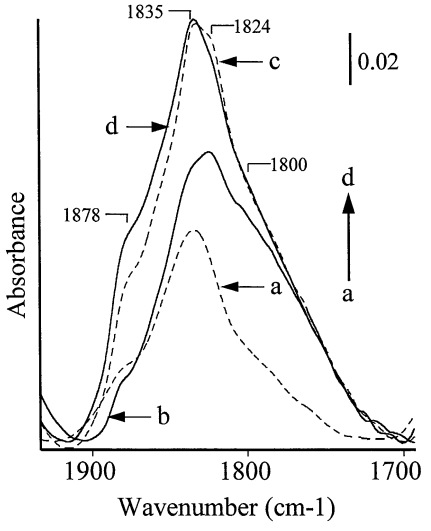

FIG. 5. Modifications of the FTIR spectra of the multibound CO species with the adsorption temperature using the 1% CO/He mixture: (a) at 300 K on the pretreated solid; (b) at 393 K; (c) at 300 K after cooling from 393 K; (d) at 300 K after a new heating to 467 K.

We have shown above (Fig. 2) that the increase in T_a from 378 to ≈500 K with the 1% CO/He mixture leads to an increase (by ≈20%) in the intensity of the IR band of the L species due probably to a reconstruction of the CO/Pt surface. A similar process is observed with the IR bands of the B and 3FC species. For instance spectrum b in Fig. 5 shows that the increase in T_a from 300 to 393 K leads to an increase in intensity of the IR. This process leads to a significant increase in the shoulder at 1800 cm^{-1} and to the better detection of the shoulder at 1824 cm^{-1}. The decrease in T_a from 393 to 300 K after the reconstruction leads to an increase in the intensity of the IR bands of the B species (Fig. 5c) while that of 3FC species is not modified. The increase in the IR bands of the B species is due to the fact that its heat of adsorption is significantly lower than those of the L and 3FC species (see below) leading to an increase in the coverage of the B species with decrease in T_a. A second increase in T_a from 300 to 467 K followed by a cooling stage to 300 K in CO/He leads to Fig. 5d which is similar to Fig. 5c, indicating that there is no more change in the CO/Pt surface (i.e., reconstruction, carbon deposition) after the first heating in 1% CO/He.

The change in the intensities of the IR bands of the B and 3FC species with T_a during this second heating stage in 1% CO/He (after the reconstruction of the CO/Pt surface) is shown in Fig. 6. The increase in T_a from 300 up to 460 K leads to a decrease in intensity of the IR bands of the B species at 1878, 1835, and 1824 cm^{-1} (Figs. 6a–6f). At 448 K, the main IR band is that of the 3FC species at 1800 cm^{-1}. Note (a) that at the opposite of the L species there is no significant

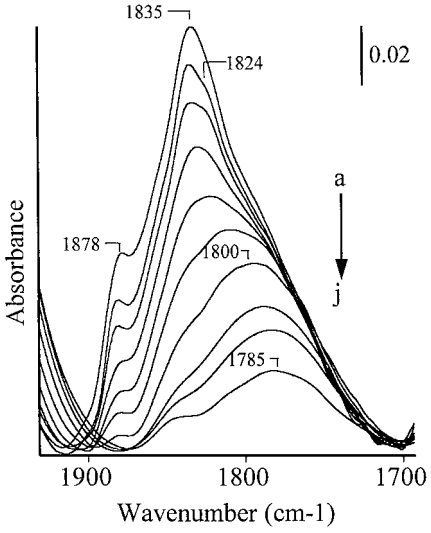

FIG. 6. Evolution of the IR bands of the multibound CO species with the adsorption temperature using the 1% CO/He mixture: (a–j) 313 K, 341 K, 366 K, 393 K, 421 K, 448 K, 478 K, 518 K, 548 K, 593 K.

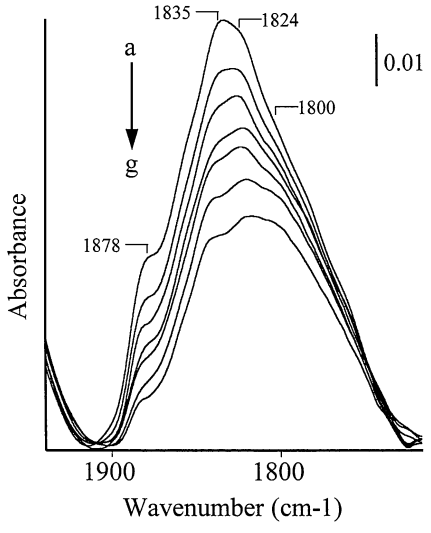

FIG. 7. Evolution of the IR bands of the multibound CO species in the course of a desorption at 300 K: (a) 1% CO/He; (b–g) in helium, 90 s, 180 s, 510 s, 600 s, 900 s, 1260 s.

shift of the IR bands of the B species with decrease in coverage and (b) the decrease in T_a from 460 to 300 K leads to a spectrum (not shown) with the same profile and intensity as that in Fig. 6a. The increase in T_a from 448 to 676 K (Figs. 6f–6j) leads to the progressive decrease in intensity of the IR band of the 3FC species alongside a shift to lower wavenumbers (1800 cm^{-1} at 478 K, 1792 cm^{-1} at 518 K, 1785 cm^{-1} at 548 K) and at $T_a > 548$ K there is no more shift. At $T_a > 448$ K, it is observed as in (21) that the broad IR band of the 3FC species splits into two components at 1845 and 1785 cm^{-1} at 593 K. However, as the intensities of the two IR bands decrease simultaneously with increase in T_a, we consider that they indicate two similar CO species and we maintain the 3FC notation. Figure 6 shows clearly that the IR bands of the B species disappear at lower temperatures than that of the 3FC species. This indicates that the heat of adsorption of the B species is significantly lower than that of the 3FC species. This is also revealed when considering the stability of the various adsorbed species during an isothermal desorption in a helium flow at 300 K after a switch 1% CO/He → He. Figure 7 shows the evolution of the IR bands as a function of the duration of the desorption. It is observed that the IR bands of the B species initially rapidly decrease and then more slowly while the broad IR band of the 3FC species is almost unaffected after more than 20 min in helium (the IR band of the L species is also not modified). This indicates that the activation energy of desorpion of the B species is lower than that of the 3FC species. The heats of adsorption of the B and 3FC species can be obtained after the determination of the contribution of each species to the evolution of the spectra in Fig. 6. This is achieved considering that, at $T_a = 548$ K only the 3FC species is present on the Pt surface, and this spectrum (with a multiplicand factor) is subtracted from those recorded at lower temperatures as shown in Fig. 8. The decrease in intensity of the IR band of the B species either in the course of the desorption at 300 K (Fig. 7) or with the increase in T_a (Fig. 6) indicates that its coverage is not equal to 1 at 300 K with a CO partial pressure of 1000 Pa. This is confirmed by Fig. 9 which shows that the intensity of the IR band of the B species increases (spectrum b) after a switch 1% CO/He → 10% CO/He due to an increase in the coverage of the B species with $P_a = 10^4$ Pa. After subtraction of the contribution of the IR band of the 3FC species from

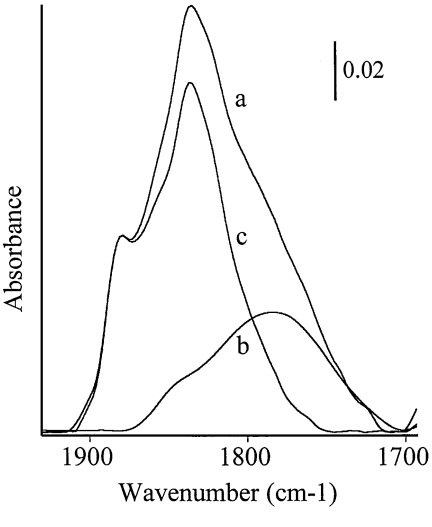

FIG. 8. Determination of the contribution of the B and 3FC adsorbed CO species to the evolution of the IR spectra with the adsorption temperature: (a) in 1% CO/He at 313 K; (b) in 1% CO/He at 483 K; (c) (spectrum a)−(spectrum b).

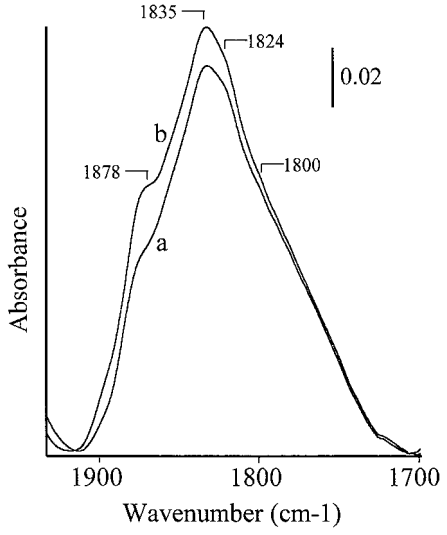

FIG. 9. Comparison of the intensities of the IR bands of the multibound CO species at 300 K with the CO partial pressure: (a) $P_a = 10^3$ Pa; (b) $P_a = 10^4$ Pa.

the spectra in Fig. 9 it is determined that the coverages of the B species at 300 K are 0.83 and 1 for the 1% CO/He and 10% CO/He mixtures, respectively. The coverages of the B and 3FC species are obtained as for the L species assuming that their respective IR band area linearly varies with the amount of each species on the surface. Studies similar to (23) to verify this assumption cannot be achieved for the B and 3FC species due to the overlap of several processes (adsorption equilibrium for B and 3FC species, reconstruction of the Pt surface, formation and decomposition of formate species on the alumina support). However, the validity of this assumption for the L species (23) supports that for the B and 3FC species. The evolution of the coverage of the B species (the three B species are not differentiated) with T_a for the 1% CO/He mixture is shown as curve c in Fig. 3. Curve d gives the evolution of the coverage of the B species with T_a using the 10% CO/He mixture (FTIR spectra not shown). Curve e in Fig. 3 gives the evolution of the coverage of the 3FC species with T_a for the 1% CO/He mixture using the results in Fig. 6 (the two IR bands at high temperatures are not differentiated). We have verified for the 3FC species that cooling of the sample in 1% CO/He after adsorption at 633 K leads to an IR band at low temperatures with a intensity only slightly lower (<10%) than the one recorded in the heating stage. Curves c–e in Fig. 3 are used for the determination of the heats of adsorption of the B and 3FC species using expressions [1] and [2].

3.4. Heats of Adsorption of the B and 3FC Species

Curve f in Fig. 3 is obtained using $E\mathrm{B}_0 = 94$ kJ/mol and $E\mathrm{B}_1 = 45$ kJ/mol, in expressions [1] and [2] with a partial pressure $P_a = 10^3$ Pa while curve g is obtained with the same heats of adsorption using $P_a = 10^4$ Pa. Note the good agreement between the theoretical and the experimental coverages of the B species for the two CO partial pressures. Curve h in Fig. 3 is obtained using $E3\mathrm{FC}_0 = 135$ kJ/mol and $E3\mathrm{FC}_1 = 104$ kJ/mol in expressions [1] and [2] for the heats of adsorption of the 3FC species and a very good agreement also is observed with the experimental data. The above results clearly show that: (a) the heats of adsorption of the B and 3FC species are lower whatever the coverage than those of the L species (i.e., at low coverages, $E\mathrm{L}_0 = 206$ kJ/mol, $E3\mathrm{FC}_0 = 135$ kJ/mol, and $E\mathrm{B}_0 = 110$ kJ/mol); (b) the difference between the heats of adsorption of the L and 3FC species decreases with increase in coverage (similar values at $\theta = 1$); and (c) there is a significant difference between the heat of adsorption of the B and the 3FC species.

The heats of adsorption of the B and 3FC species can be compared with those found in the literature on Pt containing solids using TPD and microcalorimetry methods. The difficulty in this comparison is that the heats of adsorption of individual adsorbed CO species are not reported in the literature as done above. To facilitate the discussion we compare first the present results with TPD and then with microcalorimetry studies.

3.5. Comparison of the Present Results with TPD Studies

TPD is one of the best analytical methods of revealing the presence on a metal surface of several adsorbed species with different activation energies of desorption. Numerous studies report the evolution of the TPD spectra with the coverage in CO on various Pt-containing solids. As a general trend they reveal a high-temperature TPD peak ($T_H \approx 500$ K) at low coverages, increasing with the coverage, while a second peak at lower temperatures ($T_L \approx 400$ K) appears and increases at high coverages. This has been observed: (a) on single crystals (28–41), (b) on polycrystalline platinum (filament, film, sheet) (42, 43), (c) on model Pt particles (44–46), and (d) on supported Pt catalysts (2, 47, 48). However, on supported metal catalysts the two TPD peaks, are strongly overlapped. Some studies report that T_H and T_L peaks are due to the overlap of several peaks (33, 34, 36) linked to different adsorbed CO species. Clearly, the two TPD peaks are not ascribed to L and B CO species. It seems that there is an agreement (19, 29, 39, 40) from the precursor study of Collins and Spicer (49) to consider that the two TPD peaks are linked to adsorption on steps (T_H) and on terraces (T_L). In particular, it has been shown (49) that the T_H peak is very small on smooth Pt surfaces (i.e., Pt (111)) while it was important for stepped surface. On model Pt particles Altman and Gorte (44) have shown that only the T_H peak is observed on small particles (1.1 nm) while the T_L peak is detected on large particles (>4 nm). It is commonly observed on single crystals (30–43) that only the T_H peak is observed at low coverage ($\theta \approx <0.2$) of the Pt surface while higher coverages lead to its increase and to the appearance of the T_L peak.

The assignment of the two main TPD peaks to specific adsorbed CO species is the objective of several studies using IRAS, HIRAS, and HREELS spectroscopy. For instance, on Pt (111), Steininger *et al.* (31) have shown using EELS spectroscopy that only the L species (2100 cm^{-1}) is detected at $\theta < 0.17$ and that the B species (1850 cm^{-1}) appears and increases at higher coverage. However, it is not concluded univocally that T_H and T_L peaks are due to B and L species, respectively. For instance, McClellan *et al.* (37) performed both TPD and HREELS studies on Pt(321). They observed a single IR band at 2065 cm^{-1} (L species) at low coverage ($\theta = 0.02$) while at higher coverages ($\theta > 0.08$) the IR band increased and shifted to 2095 cm^{-1} and a second IR band appeared at 1865 cm^{-1} for the B species. The authors, however (37), performed the desorption of the T_L peak leaving unchanged the T_H peak. Under these conditions both L and B species were still detected. This led the authors to attribute the T_L peak to CO adsorbed on terraces while the T_H peak was linked to CO bound to rough step sites (both L and B species). The correlation between TPD peaks and the nature of the adsorbed CO species has been particularly studied by Xu *et al.* (19, 40) on Pt(335) using TPD and IRAS (19, 40). They show that at low coverages mainly linear CO species on steps 2075 cm^{-1} are detected corresponding to the T_H peak. Then B species on steps (1880 cm^{-1}) appears followed by L species on terrace (2092 cm^{-1}) and finally B species on terrace (1900 cm^{-1}) (40). These results are in agreement with previous works performed on Pt(335) (39) and on Pt(111) (53). This leads the authors (19, 40, 39) (a) to assign the T_H peak to both L and B species on steps but with a preferential order of appearance (L followed by B), which is considered (40 and references therein) to reveal that L species on steps are more stable than B species, and (b) to consider that the T_L peak is due to both L and B species on terraces. On Pt(112) the same rule of appearance of the various adsorbed CO species is observed (19). The higher stability of the L species compared with the B species has been confirmed by several studies (50–52). In particular, Yoshinodu and Kawai (50, 51) have shown on Pt(111) that at 25 K and for $\theta = 0.1$, L species (2093 cm^{-1}) as well as B species (1871 cm^{-1}) are present on the surface but that after annealing to 150 K all the adsorbed species are linear due to their higher stability. It must be underscored that some other explanations of the two TPD peaks are proposed (54, 55).

From the above literature data it can be considered that the L species on steps have the highest heat of adsorption and we have shown above and in previous works (11, 12) that there is a reasonable agreement between the heat of adsorption of the L species determined with our procedure and the activation energy of desorption for the highest TPD peak (T_H peak) found in the literature. This is due to the fact that on the present catalyst the IR band at 2075 cm^{-1} (at 300 K) is due to L species on steps or defects (high dispersion of the Pt particles). The heats of adsorption of the B and 3FC species determined with our procedure are lower than that of the L species and this also is in agreement with the data in the literature which consider that the B species are less stable than the L species (19, 30, 39, 40, 49, 50). Moreover, we have determined that the 3FC species have a heat of adsorption higher than that of the B species in agreement with the fact that some single crystal surfaces may lead to two B species on steps and terraces with different stabilities which are linked to T_H and T_L TPD peaks, respectively (19, 39, 40). The activation energy of desorption corresponding to the T_L peak has been determined in several studies and the results are summarized in Table 1. It can be observed that at low coverage the values are 90 ± 10 kJ/mol, which are in good agreement with $EB_0 = 94$ kJ/mol. On Pt/Al_2O_3, Herz and McCready (48) observed a sharp TPD peak at low temperatures associated to broad TPD peaks at high temperatures. They determined for the low TPD peak a heat of adsorption of 74 ± 4 kJ/mol by assuming that adsorption equilibrium (Langmuir's model) conditions were maintained during the TPD experiment. We have determined that the heat of adsorption of the B species linearly varies with the coverage but it can be observed that there is an agreement between the value of (48) and the average of the heats of adsorption for the B species at high and low coverages ($EB_0 + EB_1)/2 \approx 70$ kJ/mol. The comparison of the heat of adsorption of the 3FC species with the literature data must involve the activation energy of desorption of the high TPD peak and we simplify the comparison considering that B species on step in the literature and 3FC species of the present study are similar adsorbed species. We have indicated above that some studies (33, 34, 36) point out that the high-temperature TPD peak is due to an overlap of several peaks. Considering that the E3FC must be lower than EL (19, 40), we compare the heat of adsorption of the

TABLE 1

Activation Energy of Desorption for the Low Peak ($T_H \approx 400$ K) on Various Pt-Containing Solids

Single crystal/ polycrystalline Pt	Activation energy (kJ/mol)	Frequency factor (s^{-1})	Coverage	References
Pt(111)	92	10^{13}	0.3	28
Pt(111)	100	10^{13}	>0.4	30
Pt(111)	95	10^{13}	≈0	34
Pt(110)	82	10^{13}	≈0	34
Pt(100)	99	10^{13}	≈0	34
Pt(321)	96	2.5×10^{11}	[a]	37
	109	10^{13}	[a]	
Pt(410)	92	10^{13}	[a]	36
Pt Filament	107	5×10^{11}	[a]	42
Pt sheet	104	10^{13}	[a]	43
Pt/Al_2O_3	74 ± 4	[b]	0–1	48

[a] Not indicated.

[b] Adsorption equilibrium assumption.

3FC species to the lowest activation energies obtained from T_H TPD peaks. The values are in the range 110–130 kJ/mol (33, 34, 36) (coverage not indicated) and they agree with $E3FC_0 = 135$ kJ/mol and $E3FC_1 = 104$ kJ/mol. Note that we find that L and 3FC species have similar heats of adsorption at high coverage (115 and 104 kJ/mol, respectively) in agreement with the fact that they are involved in the same T_H TPD peak. It is probably their respective amounts on the surface which leads to the detection of one or several TPD peaks at high temperatures (33, 34, 36). Finally, Xu *et al.* (19, 40) have determined on Pt(335) the following order of stability for the adsorbed CO species: L on steps > B on steps > L on terraces > B on terraces while we determine in the present study: L (on steps or defects) > 3FC > B.

3.6. Comparison of the Present Results with Microcalorimetry Studies

%This analytical procedure determines the whole heat of adsorption of CO and does not make it possible to clearly discern the contribution of the individual adsorbed species. However, taking into account the observation on single crystals (19, 39, 40) which indicates that the T_H TPD peak (mainly L species on steps) is formed at low coverages it can be considered that the microcalorimetric measurements at low coverages involve the heat of adsorption of the L species while at high coverages they involve mainly the B species with the contribution of the 3FC species at intermediate coverages. We have shown above that $EL_0 = 206$ kJ/mol is in good agreement with that (225 kJ/mol) found by Yeo *et al.* (27) using MCAC method. However, at high coverages there is a significant difference between $EL_1 = 115$ kJ/mol and the values of Yeo *et al.*: 80 kJ/mol (27). This is may be due to the fact that in (27) some adsorbed species with a low heat of adsorption (B) are formed at high coverages. Sharma *et al.* (6), using a microcalorimetric method, obtained on two Pt/SiO_2 catalysts with different metal dispersions a linear relationship between 140 kJ/mol at $\theta \approx 0$ and 100 kJ/mol at $\theta = 0.8$ and then the heat of adsorption decreases sharply to 40 kJ/mol at $\theta = 1$. For $\theta < 0.8$ the value in (6) appears as an average of the heats of adsorption which involves various parameters such as: (a) the amount of each adsorbed CO species on the surface (mainly L and 3FC at low coverages) and (b) the decrease in the heat of adsorption of each adsorbed CO species with the coverage. The strong decrease in the heat of adsorption from 100 kJ/mol at $\theta = 0.8$ to 40 kJ/mol at $\theta = 1$ observed in (6) probably indicates the adsorption of the B species. In particular, the value found in (6) at $\theta = 1$ is equal to $EB_1 = 45$ kJ/mol. Sen and Vannice (5) have determined the integral heats of adsorption of CO at high coverages on various supported Pt catalysts and Pt powders. They determined 122 ± 16 kJ/mol on dispersed Pt crystallites, a value slightly higher than on Pt powders, 112 kJ/mol. The values of Sen and Vannice are measured at a high coverage of the Pt surface, and good agreement can be observed with $EL_1 = 115$ kJ/mol and $E3FC_1 = 104$ kJ/mol found for two adsorbed CO species of the present study which probably are the main adsorbed species on the supported Pt catalysts.

Finally it appears that the heats of adsorption of individual adsorbed CO species on a Pt/Al_2O_3 obtained from the present procedure are in reasonable agreement with certain literature data. The major contribution of the present study is that we are able to clearly quantify the heats of adsorption of three adsorbed CO species (L, 3FC, B species) and their evolutions with their respective coverages. These data were not available in the literature until now.

3.7. Isosteric Heats of Adsorption of the L and B Species

Our adsorption model has been used to interpret the adsorption of L and/or B CO species on several supported metal catalysts: Pd (10), Rh (14), Ru (13), Cu (56) and this constitutes an argument to affirm that the foundational assumptions are validated. However, it is of interest to ascertain these assumptions by experimental procedures. For instance, the above heats of adsorption values can be compared with the isosteric heat of adsorption (denoted by ΔH) using the Clausius–Clapeyron equation (7). We have previously shown (12) the very good agreement between the isosteric heats of adsorption of the L species on the present Pt/Al_2O_3 catalyst and the EL values determined with the adsorption model. We have also observed the same good agreement for the L species adsorbed on a reduced Cu/Al_2O_3 catalyst (56). This comparison between ΔH and E values has been performed for the B species. The ΔH values have been obtained at several coverages from the experimental curves c and d in Fig. 3 for $P_a = 10^3$ Pa and $P_a = 10^4$ Pa, respectively. Figure 10 shows the isosteric plots

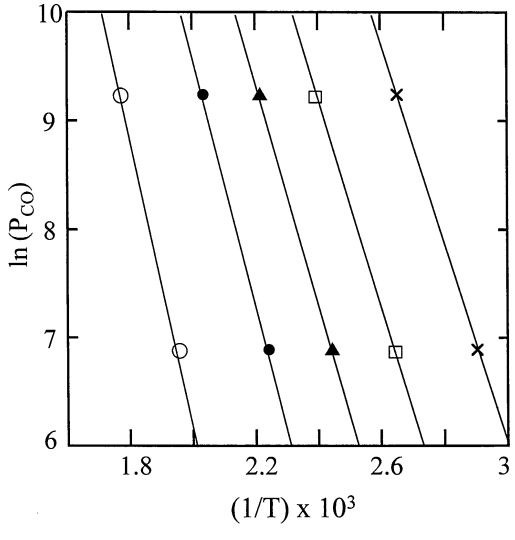

FIG. 10. Representative isosteric plots of $\ln(P_{CO})$ versus $1/T$ from the isobaric data in Fig. 3 for the B species: ×, $\theta = 0.72$; □, $\theta = 0.6$; ▲, $\theta = 0.45$; ●, $\theta = 0.32$; ○, $\theta = 0.1$.

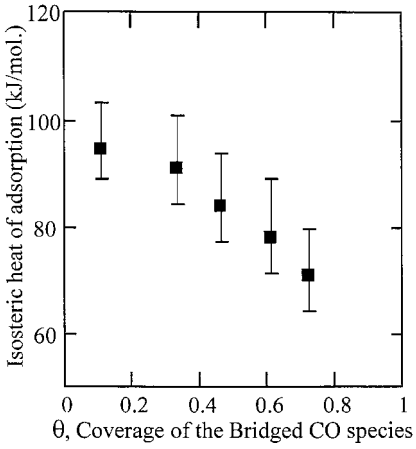

FIG. 11. Evolution of the isosteric heat of adsorption of the B CO species with the coverage and experimental uncertainties (bar graph) considering $T_a \pm 2$ K.

$\ln(P_{CO}) = f(1/T)$ for several coverages and Fig. 11 shows the evolution of $\Delta H = f(\theta)$ for the B species. It can be observed (a) that there is reasonable agreement between ΔH and the EB values; i.e., for $\theta = 0.45$ the values are $E\mathrm{B} = 72$ kJ/mol and $\Delta H = 82$ kJ/mol (this difference indicates that the frequency factors of the adsorption coefficients between the two procedures may differ by a factor of $\approx$10); and (b) that the isosteric heat of adsorption varies almost linearly with the coverage. It must be noted that the isosteric heat of adsorption values are significantly influenced by experimental uncertainties. For instance considering $T_a \pm 2$ K leads to an uncertainty on ΔH of $\approx \pm 8$ kJ/mol, as indicated in Fig. 11. The reasonable agreement between the EB and ΔH values for the B species constitutes a proof that the assumptions involved in the adsorption model are valid for this species. We have not performed the same comparison for the 3FC species because at high temperatures, with the highest CO partial pressure $P_a = 10^4$ Pa, the carbon deposition significantly affects the number of sites adsorbing the 3FC species.

4. CONCLUSIONS

The following conclusions are derived from the present study on the determination of the heat of adsorption of CO on a 2.9% Pt/Al_2O_3 catalyst.

(a) The IR spectra of the adsorbed CO species recorded under adsorption equilibrium conditions (T_a varying from 300 to 750 K with $P_a = 10^3$ Pa) can be used for the determination of the evolution of the individual coverage of three adsorbed CO species: L, B, and 3FC CO species as a function of T_a.

(b) These curves lead to the determination of the heats of adsorption of the three adsorbed species using an adsorption model.

(c) The heats of adsorption of the L CO species linearly vary with the coverage from $E\mathrm{L}_0 = 206$ kJ/mol at $\theta = 0$ to $E\mathrm{L}_1 = 115$ kJ/mol at $\theta = 1$.

(d) The heats of adsorption of the B CO species (three species with similar heats of adsorption) linearly vary with the coverage from $E\mathrm{B}_0 = 94$ kJ/mol at $\theta = 0$ to $E\mathrm{B}_1 = 45$ kJ/mol at $\theta = 1$.

(e) The heats of adsorption of the 3FC CO species linearly vary with the coverage from $E3\mathrm{FC}_0 = 135$ kJ/mol at $\theta = 0$ to $E3\mathrm{FC}_1 = 104$ kJ/mol at $\theta = 1$.

(f) For the L and B species, the corresponding E values agree with the isosteric heats of adsorption, proving that the assumptions involved in the model are valid.

The above values lead to the conclusion that in the presence of a CO partial pressure $<10^3$ Pa (in the range of that found in exhaust gas) and for an adsorption temperature >300 K, some Pt sites of the 2.9% Pt/Al_2O_3 catalyst are still not fully covered even at low temperatures (i.e., Pt sites for the adsorption of the B CO species) and are partially free, without any competition, for the adsorption of a second reactant gas together with CO.

ACKNOWLEDGMENT

We acknowledge with pleasure the FAURECIA Company, Bois sur prés 25 550 Bavans, France, for its financial support and the M.E.R.T (Ministère de l'Education Nationale, de la Recherche et de la Technologie) for the research fellowship of A. Bourane.

REFERENCES

1. Boudart, M., *in* "Handbook of Heretogeneous Catalysis" (G. Ert, H. Knözinger, and J. Weitkamps, Eds.), Vol. 1. Wiley, New York, 1997.
2. Sachtler, W. M. H., *in* "Handbook of Heretogeneous Catalysis" (G. Ert, H. Knözinger, and J. Weitkamps, Eds.), Vol. 3. Wiley, New York, 1997.
3. Demmin, R. A., and Gorte, R. J., *J. Catal.* **90**, 32 (1984).
4. Herz, R. K., Kiela, J. B., and Marin, S. P., *J. Catal.* **73**, 66 (1982).
5. Sen, B., and Vannice, M. A., *J. Catal.* **130**, 9 (1991).
6. Sharma, S. B., Miller, J. T., and Dumesic, J. A., *J. Catal.* **148**, 198 (1994).
7. Tompkins, F. C., "Chemisorption of Gases on Metal." Academic Press, London, 1978.
8. Kuhn, W. K., Szanyi, J., and Goodman, D. W., *Surf. Sci.* **303**, 377 (1994).
9. Kuhn, W. K., Szanyi, J., and Goodman, D. W., *Surf. Sci.* **274**, L611 (1992).
10. Dulaurent, O., Chandes, K., Bouly, C., and Bianchi, D., *J. Catal.* **188**, 237 (1999).
11. Chafik, T., Dulaurent, O., Gass, J. L., and Bianchi, D., *J. Catal.* **179**, 503 (1998).
12. Dulaurent, O., and Bianchi, D., *Appl. Catal. A* **196**, 271 (2000).
13. Dulaurent, O., Nawdali, M., Bourane, A., and Bianchi, D., *Appl. Catal. A* **201**, 271 (2000).
14. Dulaurent, O., Chandes, K., Bouly, C., and Bianchi, D., *J. Catal.* **192**, 261 (2000).
15. Barth, R., Pitchai, R., Anderson, R. L., and Verykios, X. E., *J. Catal.* **116**, 61 (1989).
16. Primet, M., Basset, J. M., Mathieu, M. V., and Prettre, M., *J. Catal.* **29**, 213 (1973).

17. Jackson, S. D., Glanville, B. M., Willis, J., McLellan, G. D., Webb, G., Moyes, R. B., Simpson, S., Wells, P. B., and Whyman, R., *J. Catal.* **139**, 207 (1993).
18. Vaarkamp, M., Miller, J. T., Modica, F. S., and Nieuwenhuys, D. C., *J. Catal.* **163**, 310 (1996).
19. Xu, J., and Yates, J. T., Jr., *Surf. Sci.* **327**, 193 (1995).
20. Vannice, M. A., and Twu, C. C., *J. Chem. Phys.* **75**, 5944 (1981).
21. Hayden, B. E., and Bradshaw, A. M., *Surf. Sci.* **125**, 787 (1983).
22. Haaland, D. M., *Surf. Sci.* **185**, 1 (1987).
23. Bourane, A., Dulaurent, O., and Bianchi, D., *J. Catal.* in press.
24. Glasstone, S., Laidler, K. J., and Eyring, H., *in* "The Theory of Rate Processes." McGraw-Hill, NY and London, 1941.
25. Laidler, K. J., *Catalysis* **1**, 75 (1954).
26. Liao, M. S., Cabrera, C. R., and Ishikawa, Y., *Surf. Sci.* **445**, 267 (2000).
27. Yeo, Y. Y., Wartnaby, C. E., and King, D. A., *Science* **268**, 1731 (1995).
28. McCabe, R. W., and Shmidt, L. D., *Surf. Sci.* **65**, 189 (1977).
29. Ertl, G., Neumann, M., and Streit, K. M., *Surf. Sci.* **64**, 393 (1977).
30. Norton, P. R., Goodale, J. W., and Selkirk, E. B., *Surf. Sci.* **83**, 189 (1979).
31. Steininger, H., Lehwald, S., and Ibach, H., *Surf. Sci.* **123**, 264 (1982).
32. Thiel, P. A., Behm, R. J., Norton, P. R., and Ertl, G., *J. Chem. Phys.* **78**, 7448 (1983).
33. Barteau, M. A., Ko, E. I., and Madix, R. J., *Surf. Sci.* **102**, 99 (1981).
34. McCabe, R. W., and Schmidt, L. D., *Surf. Sci.* **66**, 101 (1977).
35. Hofmann, P., Bare, S. R., and King, D. A., *Surf. Sci.* **117**, 245 (1982).
36. Park, Y. O., Banholzer, W. F., and Masel, R. I., *Surf. Sci.* **155**, 341 (1985).
37. McClellan, M. R., Gland, J. L., and McFeeley, F. R., *Surf. Sci.* **112**, 63 (1981).
38. Henderson, M. A., Szabo, A., and Yates, J. T., Jr., *J. Chem. Phys.* **91**, 7245 (1989).
39. Luo, J. S., Tobin, R. G., Lambert, D. K., Fisher, G. B., and DiMaggio, C. L., *Surf. Sci.* **274**, 53 (1992).
40. Xu, J., Henriksen, P. N., and Yates, J. T., Jr., *Langmuir* **10**, 3663 (1994).
41. Hayden, B. E., Kretzschmar, K., Bradshaw, A. M., and Greenler, R. G., *Surf. Sci.* **149**, 394 (1985).
42. Winterbottom, W. L., *Surf. Sci.* **37**, 195 (1973).
43. Collins, D. M., Lee, J. B., and Spicer, W. E., *Surf. Sci.* **55**, 389 (1976).
44. Altman, E. I., and Gorte, R. J., *Surf. Sci.* **172**, 71 (1986).
45. Zafiris, G. S., and Gorte, R. J., *Surf. Sci.* **276**, 86 (1992).
46. Zhu, Y., and Schmidt, L. D., *Surf. Sci.* **129**, 107 (1993).
47. Foger, K., and Anderson, J. R., *Appl. Surf. Sci.* **2**, 335 (1979).
48. Herz, R. K., and McCready, D. F., *J. Catal.* **81**, 358 (1983).
49. Collins, D. M., and Spicer, W. E., *Surf. Sci.* **69**, 85 (1977).
50. Yoshinobu, J., and Kawai, M., *Surf. Sci.* **363**, 105 (1996).
51. Kawai, M., and Yoshinobu, J., *Surf. Sci.* **368**, 239 (1996).
52. Fukutani, K., Magkoev, T. T., Murata, Y., and Terakura, K., *Surf. Sci.* **363**, 185 (1996).
53. Mieher, W. D., Whitman, L. J., and Ho, W., *J. Chem. Phys.* **91**, 3228 (1986).
54. Sharma, R. K., Brown, W. A., and King, D. A., *Surf. Sci.* **414**, 68 (1998).
55. Banholzer, W. F., Parise, R. E., and Masel, R. I., *Surf. Sci.* **155**, 653 (1985).
56. Dulaurent, O., Courtois, X., Perrichon, V., and Bianchi, D., *J. Phys. Chem.* **B104**, 6001 (2000).